Journal of Molecular Graphics and Modelling 29 (2010) 498–505

Contents lists available at ScienceDirect

Journal of Molecular Graphics and Modelling

journal homepage: www.elsevier.com/locate/JMGM

Theoretical study on the electronic absorption spectra and molecular orbitals of ten novel ruthenium sensitizers derived from N3 and K8

Ping Guo [a], Ruimin Ma [a], Lianshun Guo [a], Linlin Yang [a], Jifeng Liu [a], Xianxi Zhang [a,*], Xu Pan [b,**], Songyuan Dai [b,**]

[a] School of Chemistry and Chemical Engineering, Liaocheng University, 1# Hunan Road, Liaocheng, Shandong 252059, China
[b] Division of Solar Energy Materials and Engineering, Institute of Plasma Physics, Chinese Academy of Sciences, P.O. Box 1126, Hefei, Anhui 230031, China

ARTICLE INFO

Article history:
Received 24 May 2010
Received in revised form
29 September 2010
Accepted 4 October 2010
Available online 12 October 2010

Keywords:
Dye-sensitized solar cells
DFT calculations
Molecule design
Orbital energy level
Electronic absorption spectra

ABSTRACT

Ten novel sensitizer candidates Ru2, Ru4, Ru5, Ru6, Ru7, Ru8, Ru9, Ru10, Ru11 and Ru12 derived from the sensitizers N3 and K8 were designed and studied using the density functional theory and time-dependent density functional theory calculations. The influences of the C=C double bonds between the carboxyl groups and the bipyridine ring as well as the numbers and positions of the –CN groups adjacent to the carboxyl groups on the properties of the sensitizer candidates were discussed. The energy levels and the spatial distributions of the frontier molecular orbitals as well as the electronic absorption spectra of these complexes were compared with those of N3 and K8. Ru10 and Ru7 were found promising to provide superior photon-to-current conversion efficiency to those of N3 and K8 in ruthenium complex sensitized solar cells.

1. Introduction

Dye-sensitized solar cells (DSSCs) have attracted significant attention over the past decade [1–7]. The dye used in these cells is one of the key components for high power conversion efficiencies. Cis-di(thiocyanato)bis(2,2′-bipyridyl-4,4′-dicarboxylate)ruthenium(II) (N3) reported in 1993 has been found an efficient sensitizer for DSSCs [8]. Overall energy conversion efficiencies greater than 10% and incident photon-to-current conversion efficiencies (IPCE) of 80–85% under air mass (AM) 1.5 irradiation have been obtained using N3 sensitizer [8–10]. It also has high photo and chemical stability. N3 is thus often considered as a standard dye for comparison with other novel sensitizers in DSSC devices. However, the energy conversion efficiency of N3 is still not high enough. Further design of better sensitizers to improve the energy conversion efficiency is still very important in this field.

The ideal sensitizer for a single junction photovoltaic cell should meet several requirements: (i) it should absorb all light below a threshold wavelength of about 920 nm, (ii) it must also carry attachment groups such as carboxylate or phosphonate to firmly graft it to the TiO_2 surface, (iii) it should inject electrons into the solid with a high quantum yield of unity and (iv) it should be stable enough under long term illumination [2]. The lowest unoccupied molecular orbital (LUMO) and the highest occupied molecular orbital (HOMO) of the dye designed are also expected to be maintained at levels where the photo-induced electron transfer into the TiO_2 conduction band and the regeneration of the dye by iodide can take place at practically 100% yield [2].

The main drawback of N3 sensitizer is the lack of absorption in the red region of the visible spectrum and also the relatively lower molar extinction coefficient [8]. Many approaches have been tried to overcome these shortcomings since it was reported in 1993. There are four main directions to modify the structures of the dye molecules. One way is to change one of the 4,4′-dicarboxyl-2,2′-bipyridine ligand into a bipyridine ligand with electron-donating groups, which was mostly studied in the past decade [11–16]. The second way is to extend the π-conjugation ring system of the carboxyl-substituted ligand [17–21]. The third way is to replace the NCS^- with other anions, which was also widely studied [8,22–25]. The fourth way is to extend the π-conjugation bridge between the carboxylate and the ligand ring, which was rarely studied [16,26]. Further research along this direction may lead to novel progress in this field.

Combined experimental and computational studies of several ruthenium sensitizers originated from N3 have been reported [27–31]. Zinc phthalocyanine and porphyrin sensitizers were also studied using computational method [32–35]. These works all

* Corresponding author. Tel.: +86 635 8230680; fax: +86 635 8239121.
** Corresponding authors.
E-mail addresses: zhangxianxi@lcu.edu.cn, xxzhang3@gmail.com (X. Zhang).

1093-3263/$ – see front matter © 2010 Elsevier Inc. All rights reserved.
doi:10.1016/j.jmgm.2010.10.002

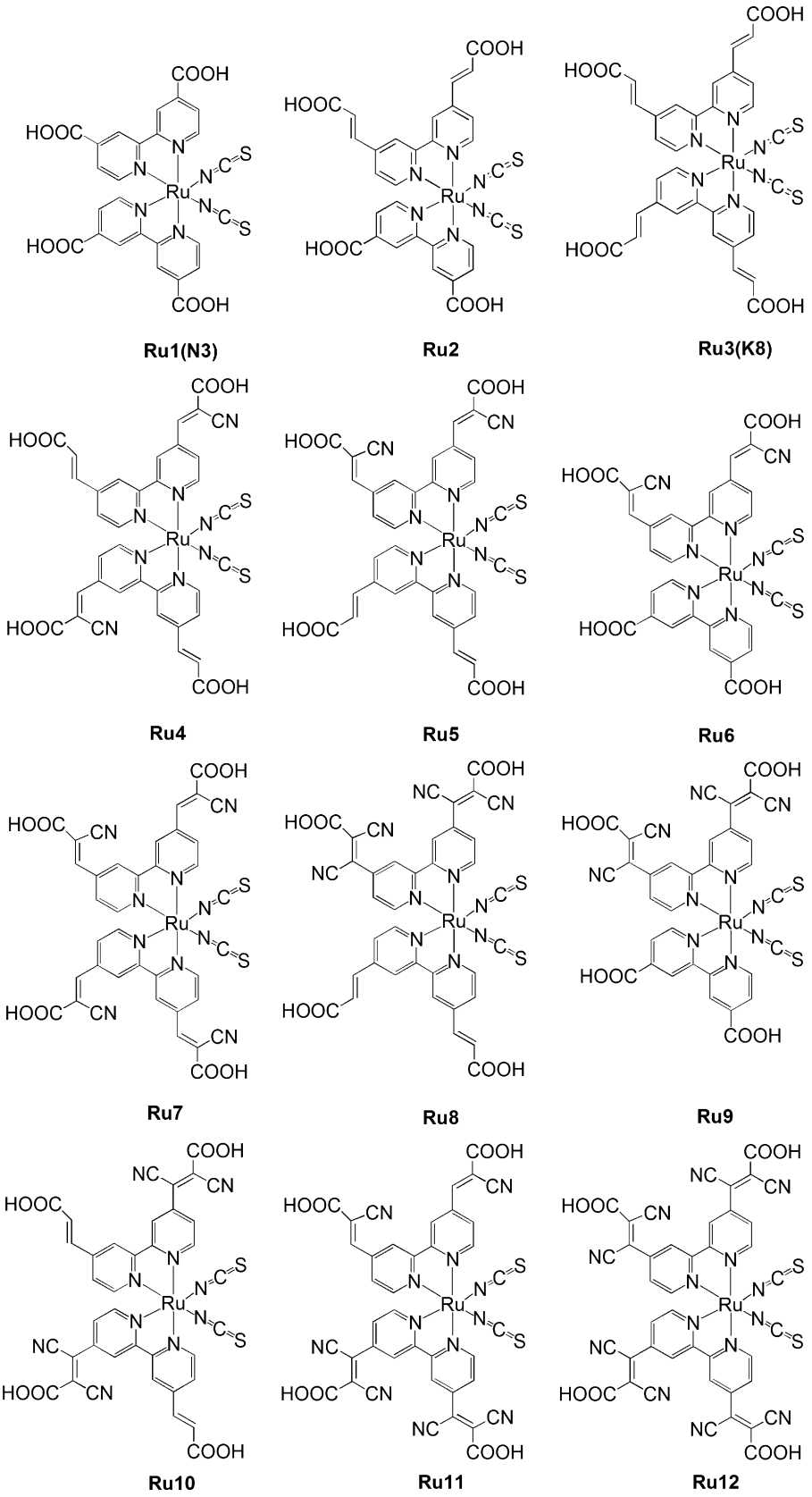

Fig. 1. Molecular structures of N3, K8 and the novel candidates designed.

certify that the simulated electronic absorption spectra and the experimental data are well correlated both in terms of the band positions and the relative intensity. The molecular orbitals and the electronic absorption spectra of the sensitizers calculated can provide additional insights into the electronic factors governing the efficiency of dye-sensitized solar cells. Computational study is thus very useful and feasible to predict the property of novel sensitizer candidates designed for dye-sensitized solar cells.

Table 1
Major bond lengths (Å) of N3 calculated using three different basis sets and the crystal data.

Parameters	Experimental[a]	LANL2DZ/6-31G*	3-21G*	LANL2DZ
$R_{Ru\text{-}NCS}$	2.048(12)–2.046(16)	2.057(70)–2.057(62)	2.050(59)–2.050(52)	2.046(93)–2.046(92)
$R_{Ru\text{-}bpycis}$	2.036(15)–2.058(12)	2.085(26)–2.085(31)	2.072(58)–2.072(65)	2.056(97)–2.056(98)
$R_{Ru\text{-}bpytrans}$	2.030(13)–2.013(14)	2.081(50)–2.081(71)	2.073(59)–2.073(76)	2.065(48)–2.065(52)
$R_{N\text{-}C(NCS)}$	1.162(21)–1.103(27)	1.185(25)–1.185(25)	1.188(73)–1.188(73)	1.197(09)–1.197(09)
$R_{S\text{-}C(NCS)}$	1.615(18)–1.685(22)	1.628(35)–1.628(36)	1.622(30)–1.622(31)	1.671(59)–1.671(59)

[a] Cited from Refs. [27,39].

$[Ru(II)L_2(NCS)_2]$ (K8, L = 4,4′-bis(carboxyvinyl)-2,2′-bipyridine) has been designed with the main absorption bands 20 nm red shifted and the molar extinction coefficient 30% increased as compared with those of N3 [26]. This improvement is mainly attributed to the additional vinylene group introduced between the carboxyl group and the bipyridine ring. The energy conversion efficiency of the primarily optimized K8-sensitized solar cell is 8.64%, which is comparable to that of N3. Further modification of K8 may lead to better performance.

The HOMO–LUMO gap of the sensitizer should be decreased in order to push the absorption band to the longer wavelength side, which means the LUMO should be lowered. The NCS^- acts as donor and the di-carboxyvinyl-bipyridine the acceptor for K8. It was considered helpful to lower the LUMO level with additional –CN groups being added to the vinylene group adjacent to the carboxyl group according to our previous research [32–35]. One novel ruthenium complex was designed with double bonds inserted between the carboxyl groups and the bipyridine ring in one ligand (Ru2) as shown in Fig. 1. This complex forms a series together with N3 and K8 to provide information about influences of different numbers of C=C double bonds on the properties of the sensitizers. Nine other novel ruthenium complexes were designed based on Ru2 and K8 with different numbers of –CN groups attached to different positions of the di-carboxyvinyl-bipyridine to provide information about influences of different numbers of –CN groups and C=C double bonds on the properties of the sensitizers.

2. Computational method

Density functional theory (DFT) and time-dependent density functional theory (TDDFT) calculations at B3LYP level using 3-21G* [27–29,36], LANL2DZ [27,30,31,37] basis sets and a hybrid LANL2DZ/6-31G* basis set [37,38] were performed to simulate the molecular structure and the UV–vis absorption spectrum of the N3 dye. The central Ru ion was considered as Ru^{2+} in this case, with the electronic configuration of $4d^6$. The bipyridine is strong field ligand so that the d electron distribution in the Ru ion is low spin, and thus all six d electrons of Ru^{2+} are paired and no single electron left. The spin multiplicity of the central Ru ion was thus set as 1 in these and the following calculations. The agreement of the calculated results with the experiment data [8,27,39] obtained using the 3-21G* basis set were found comparable to that of LANL2DZ while better than that of LANL2DZ/6-31G* besides the large benefit of time saving, which was therefore adopted in the following calculations. K8 and the novel candidates designed were then calculated at density functional B3LYP level using the 3-21G* basis set for both geometry optimizations and frequency calculations. The structures of the complexes were optimized with no symmetry constraints. The same functional and basis set were also used for TDDFT calculations to simulate the electronic absorption spectra of these complexes in ethanol. The solvent effect was evaluated using the polarizable continuum model (PCM) [40]. All calculations were carried out using the Gaussian 03 program [41] on the IBM P690 system in Shandong Province High Performance Computer Center.

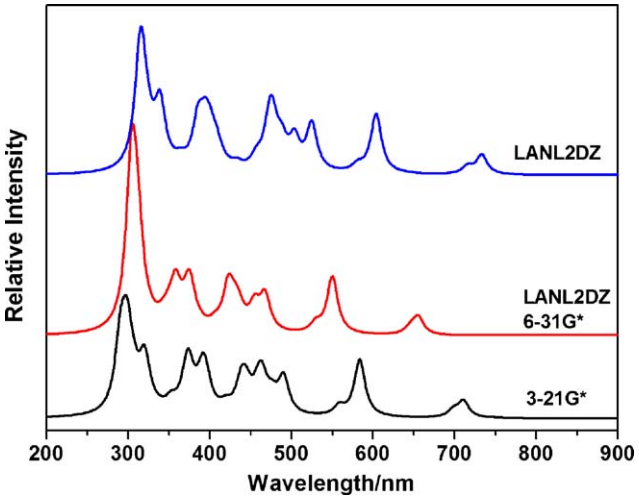

Fig. 2. Electronic absorption spectra of N3 simulated using three different basis sets.

3. Results and discussion

3.1. Comparison of the calculation results of N3 using three different basis sets

No imaginary vibration was predicted in the frequency calculations, indicating that the energy minimum structures of N3 are true energy minima. The major molecular structure parameters of N3 calculated using LANL2DZ/6-31G*, LANL2DZ and 3-21G* basis sets are listed in Table 1 comparatively with the crystal structure data [27,39]. The agreement of the calculated results with the experiment data [27,39] obtained using the 3-21G* basis set were found comparable to that of LANL2DZ while better than that of LANL2DZ/6-31G* besides the large benefit of time saving, which was therefore adopted in the following calculations.

The simulated electronic absorption spectra using these three different basis sets are shown in Fig. 2 and corresponding electronic excitation energies are listed in Table 2 together with the experimental data [8]. The agreement of the calculated results with the experiment data [8] obtained using the 3-21G* basis set was also found comparable to that of LANL2DZ while better than that of

Table 2
Electronic excitation energies (eV) of N3 obtained from the experimental data and those calculated using three different basis sets.

N3	I	II	III
Experimental[a]	2.38(1.0)	3.18(1.0)	3.97(–)
3-21G*	2.12(0.118)	3.14(0.056)	3.87(0.101)
	2.52(0.074)	3.32(0.097)	
LANL2DZ/6-31G*	2.05(0.122)	3.46(0.085)	4.08(0.267)
	2.25(0.118)	3.98(0.076)	
LANL2DZ	2.05(0.122)	3.22(0.089)	3.94(0.186)
	2.36(0.096)	3.66(0.120)	

[a] Cited from Ref. [8].

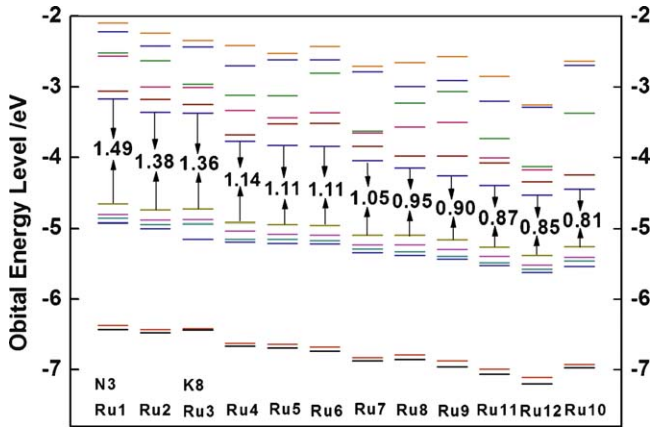

Fig. 3. Orbital energy levels of N3, K8 and the novel candidates designed.

LANL2DZ/6-31G* besides the large benefit of time saving. The 3-21G* basis set was therefore adopted in the following calculations.

3.2. Molecular orbital energy levels of N3, K8 and the novel candidates designed

No imaginary vibration was predicted in the frequency calculations, indicating that the energy minimum structures of K8 and the novel candidates designed are also true energy minima. Referring to previous theoretical studies of ruthenium complexes [27–31], the orbital energy levels of the first six highest occupied molecular orbitals, the first six lowest unoccupied molecular orbitals and the HOMO–LUMO gaps of N3, K8 and ten novel candidates designed are shown in Fig. 3. The molecular orbital energy levels were found decrease from N3 to Ru10. The patterns of the occupied orbitals for all these twelve complexes considered are qualitatively similar. The six highest occupied molecular orbitals can be divided into two subgroups. The HOMO to HOMO-3 lying within 0.42 eV have essentially ruthenium t_{2g} character [29] with sizable contribution coming from the NCS^- ligand orbital, which can also be observed from the molecular orbital spatial distributions shown in Fig. 4. The HOMO-4 and HOMO-5 of these twelve sensitizers considered are almost degenerate lying within 0.09 eV.

The lowest unoccupied molecular orbitals of the complexes investigated are a set of bipyridine π^* orbitals [29], which have different localizations depending on the substituents attached to the bipyridine ring. The first six lowest unoccupied molecular orbitals of N3 and K8 can be divided into three couples that are very close, in which the LUMO/LUMO+1, LUMO+2/LUMO+3, LUMO+4/LUMO+5 couples are essentially localized over the pyridines with the carboxyl and carboxyvinyl groups, respectively. The stabilization of the π^* orbitals localized on the pyridine ligands with the carboxyl groups is a common feature of all these N3-derived dyes. This should favor the electron injection from the dye to the semiconductor surface. The molecules designed in this work show some differences in the unoccupied orbitals, which results in reductions of the HOMO–LUMO gaps in different extents. This may be attributed to the fact that the two bipyridine ligands of the novel sensitizers are not equivalent. The HOMO energy level of N3 is located at −4.66 eV, which is about 0.07 eV above that of K8. The LUMO energy level of N3 is located at −3.17 eV, which is about 0.20 eV above that of K8. K8 thus has a narrower HOMO–LUMO gap than that of N3.

Ru1, namely N3, has the largest HOMO–LUMO gap 1.49 eV and Ru10 the smallest gap 0.81 eV among these twelve molecules. The HOMO–LUMO gap of Ru6 was found 0.27 eV reduced with two –CN groups added comparing with that of Ru2. 0.21 eV reduction was also observed similarly between the HOMO–LUMO gaps of Ru6 and Ru9. Ru4 and Ru5 have different HOMO–LUMO gaps because the two –CN groups are attached to different positions of the dicarboxyvinyl-bipyridine. This is also same to Ru7, Ru8 and Ru10, which all have four –CN groups while different HOMO–LUMO gaps 1.05 eV, 0.95 eV and 0.81 eV, respectively. The HOMO–LUMO gaps decrease along with increasing the numbers of the –CN groups from

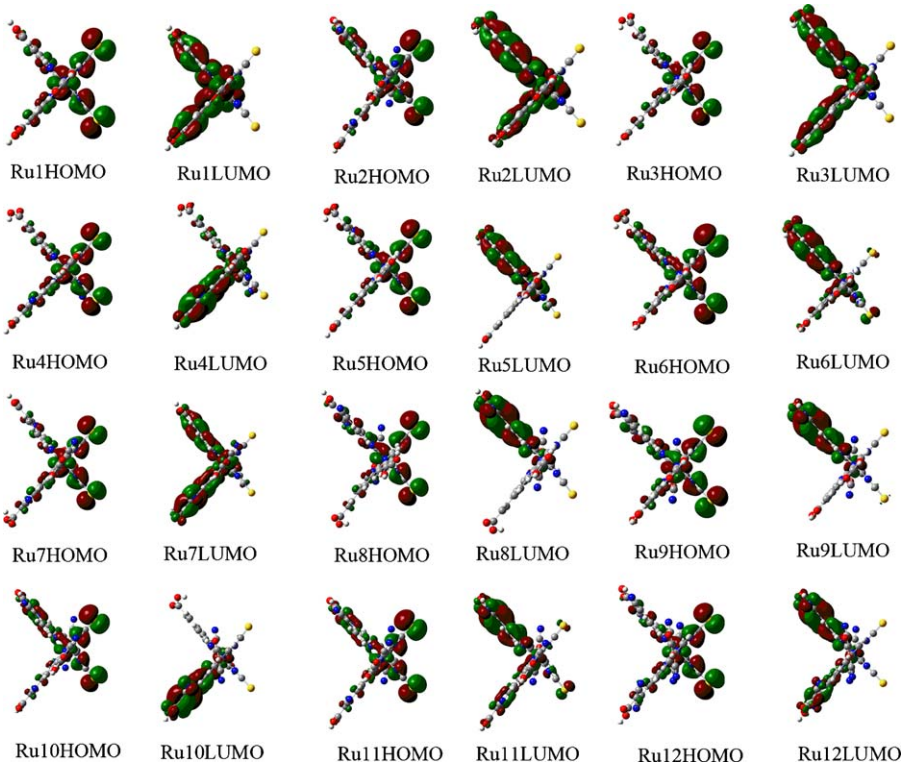

Fig. 4. Molecular orbital distributions for N3, K8 and ten novel candidates designed.

Ru3, Ru4, Ru8, Ru11 to Ru12. In general, the HOMO–LUMO gaps tend to decrease along with increasing the numbers of the –CN groups.

The narrower HOMO–LUMO gap is benefit for absorbing the longer-wavelength light. More photons can thus be absorbed at the same time, which may contribute to obtain higher short circuit current density J_{sc} and further higher photon-to-electricity conversion efficiency η. The novel sensitizers designed except Ru2 all have lower LUMO levels and smaller HOMO–LUMO gaps than those of K8 and N3, indicating that absorption bands at even longer wavelength side as well as higher J_{sc} and η may be obtained.

3.3. Electronic structures of N3, K8 and the novel candidates designed

Mizuseki et al. [42] suggested that the charge transport was also related to the spatial distribution and the composition of the frontier orbitals. In order to get more information about these molecules, the compositions and spatial distributions of the HOMO and LUMO for N3, K8 and ten novel candidates designed were also calculated. The spatial distributions of the HOMO and LUMO for these complexes are shown in Fig. 4. The HOMO of N3 shows contributions from the ruthenium ion and the isothiocyanate ligands. The LUMO of N3 is a π^* orbital delocalized mostly over the bipyridine ring with sizable contributions from the carboxyl groups, which corresponds well with previous report [29]. This indicates that the photoexcited electron is transferred from the metal ion and the NCS^- to the bipyridine ligand, which is of benefit to the injection of the photo excited electrons to the conduction band of the semiconductor.

The C=C double bonds inserted between the bipyridine ring and the anchoring groups as well as the –CN substituents introduced adjacent to the carboxyl groups decrease the HOMO–LUMO gaps and move the LUMO more localized at the acceptor section as shown in Fig. 4, which may further increase the efficiency of the charge-separated state. More detailed discussion is provided based on the frontier molecular orbital compositions as follows.

The typical ruthenium complexes used as sensitizers in DSSCs mostly have Ru^{2+} and NCS^- as donors and the carboxyl-containing groups as acceptors. The charge transfer orientation is associated with the difference between the HOMO of the donor and the LUMO of the acceptor, which is an important factor that affects the electron injection efficiency. The HOMO of these twelve complexes are mainly composed of the ruthenium ion and the ligand NCS^-, while the LUMO the carboxyl-containing groups. If Ru^{2+} and NCS^- of the molecule have higher proportion in HOMO and the acceptor has higher proportion in LUMO, then the sensitizer would be more likely to have higher photon-to-current conversion efficiency.

The compositions of the HOMO and LUMO for N3, K8 and these ten novel complexes are listed in Table 3. Ru^{2+} of K8 and the ten novel ruthenium complexes have a little lower proportions in the HOMO than that of N3. NCS^- of Ru2 and Ru6 have higher proportion

Table 3
The orbital compositions of the twelve ruthenium complexes.

	Orbital	Ru	NCS	COOH	CN	Acceptor
N3(Ru1)	HOMO	25.2%	32.8%	0.20%	–	4.60%
	LUMO	6.96%	0.727%	3.02%	–	45.8%
Ru2	HOMO	19.3%	35.0%	0.177%	–	5.09% 5.61%(C=C)
	LUMO	7.75%	0.930%	2.15%	–	13.4% 77.0%(C=C)
K8(Ru3)	HOMO	25.0%	30.9%	0.15%	–	6.6%
	LUMO	5.98%	0.73%	1.89%	–	46.28%
Ru4	HOMO	22.9%	32.7%	1.39%	0.15%	5.85%
	LUMO	6.59%	0.94%	2.00%	2.80%	45.8%
Ru5	HOMO	21.0%	32.9%	0.20%	0.25%	3.83% 8.07%(2CN)
	LUMO	10.8%	2.03%	3.02%	3.17%	5.16% 61.6%(2CN)
Ru6	HOMO	17.2%	34.3%	0.218%	0.260%	4.23% 9.97%(2CN)
	LUMO	9.46%	2.10%	1.93%	3.15%	4.74% 81.6%(2CN)
Ru7	HOMO	21.3%	32.1%	0.18%	0.34%	7.25%
	LUMO	4.15%	0.90%	1.94%	3.34%	47.0%
Ru8	HOMO	21.3%	31.6%	0.221%	0.263%	3.74% 11.8%(4CN)
	LUMO	10.4%	2.56%	2.04%	3.31%	3.55% 80.9%(4CN)
Ru9	HOMO	17.2%	32.5%	0.284%	0.354%	3.53% 14.27%(4CN)
	LUMO	9.44%	3.11%	1.86%	3.79%	2.41% 81.93%(4CN)
Ru10	HOMO	20.8%	30.0%	0.331%	0.507%	9.6%
	LUMO	1.96%	0.708%	2.12%	4.00%	48.3%
Ru11	HOMO	20.7%	30.9%	0.238%	0.229%	4.78%(2CN) 12.7%(4CN)
	LUMO	7.82%	2.19%	1.85%	2.47%	8.64%(2CN) 79.16%(4CN)
Ru12	HOMO	20.9%	30.4%	0.252%	0.194%	9.15%
	LUMO	2.92%	0.865%	2.10%	1.93%	47.7%

Table 4
The most representative excitation energies (ΔE), absorption wavelength, oscillator strengths (f), and dominant excitation character of N3 and K8 in ethanol.

N3						K8					
State	Main configuration		ΔE (eV) and λ (nm)	f	Exp (eV)[a]	State	Main configuration		ΔE (eV) and λ (nm)	f	Exp (nm)[b]
1	175 → 179	40%	2.12(584)	0.118		1	205 → 206	86%	1.10(728)	0.056	
	176 → 178	41%			2.38	5	203 → 206	43%	2.06(602)	0.180	
7	177 → 180	92%	2.52(490)	0.074		7	205 → 208	80%	2.22(558)	0.160	555
9	174 → 178	59%	2.67(464)	0.060		10	203 → 208	69%	2.49(497)	0.113	439
15	177 → 182	68%	2.83(438)	0.052		21	200 → 206	38%	3.10(400)	0.050	
19	172 → 178	91%	3.14(394)	0.056	3.18	22	200 → 206	30%	3.11(399)	0.052	
25	171 → 178	85%	3.32(374)	0.097		23	202 → 209	55%	3.13(397)	0.078	
34	172 → 180	61%	3.87(320)	0.101	3.97	27	199 → 206	88%	3.26(381)	0.098	
46	170 → 178	37%	4.16(298)	0.063		30	200 → 208	36%	3.54(350)	0.179	326
49	169 → 179	57%	4.26(291)	0.066			201 → 209	36%			
50	176 → 186	30%	4.27(290)	0.063		44	193 → 206	21%	4.00(310)	0.088	312
						45	194 → 206	19%	4.00(309)	0.146	
							200 → 210	21%			
						49	200 → 210	29%	4.11(302)	0.156	

[a] Cited from Ref. [27].
[b] Cited from Ref. [26].

in the HOMO than that of N3. NCS^- of Ru4, Ru5, Ru7 and Ru9 have similar proportion in the HOMO to that of N3 at around 32.8%. NCS^- of the other novel molecules have a little lower proportion in the HOMO than that of N3. The acceptor of Ru4 has an equal proportion in the LUMO compared with that of N3. The acceptors of the other nine novel complexes all have higher proportion in the LUMO than that of N3. This shows that the LUMO are much more moved to the acceptor moieties, which indicates that more efficient electron injection may be obtained using the novel sensitizer candidates designed.

3.4. Electronic absorption spectra of N3, K8 and the novel candidates designed

The wavelengths, oscillator strengths, transition energies and molecular orbital excitations for the most relevant transitions of N3, K8 and the novel candidates designed were obtained through TDDFT calculations in ethanol, which was often used as solvent in previous experimental research works [8,29]. The electronic absorption spectra were simulated by fitting to a Lorentzian line shape with a half-width at half-maximum of 8 nm. The experimental and theoretical absorption spectra data of N3 and K8 in ethanol are listed comparatively in Table 4. The simulated electronic absorption spectra of N3, K8 and the novel candidates designed are shown in Figs. 5 and 6. It should be noted that the calculated oscillator strengths of molecular orbital transitions do not always match the absorbance measured experimentally, the relative intensities of the absorption bands for these compounds could be used as only a qualitative reference rather than a quantitative index.

The experimental spectrum of N3 shows three main features, which are well reproduced in the spectrum simulated as shown in Table 4. The first experimental absorption band at 2.38 eV was reflected in the spectrum simulated at 2.12 eV and 2.52 eV [27]. The intense band at 3.97 eV in experiment was calculated at 3.87 eV. The experimental absorption bands at 555 and 439 nm of K8 [26] were calculated at 558 and 497 nm, respectively. There are two high-energy bands at 312 and 326 nm in the experimental data [26], which are calculated at 310 and 350 nm, respectively. The agreement between theory and experiment is good, which indicates that the B3LYP functional combined with the 3-21G* basis set provides an effective measure to predict the absorption spectra of the novel ruthenium complexes.

The absorption spectra of Ru1, Ru2 and Ru3 seem similar as shown in Fig. 5. The absorption intensity is increased from Ru1 to Ru3. The absorption spectrum of Ru2 is 10 nm red-shifted comparing with Ru1 (N3). The absorption spectrum of Ru3 (K8) is 10 nm red-shifted comparing with Ru2. This shows that the absorption intensity is increased and the absorption positions is red-shifted along with the increasing numbers of the C=C double bonds between the carboxyl groups and the bipyridine ring, which agrees well with the experimental results of N3 and K8 [8,26].

Comparing the simulated spectra of Ru2, Ru6 and Ru9 which have the same number of C=C double bonds and different numbers of –CN groups shown in Fig. 5, the absorption intensities are decreased and the absorption positions are red-shifted from Ru2 to Ru9. The C=C double bond can increase the absorption intensity and make the absorption positions slightly red-shift, however, the –CN group is somewhat opposite. The introduction of the –CN groups to the molecules investigated make the absorption positions significantly red-shifted while the absorption intensities decreased.

The maximum absorption wavelength calculated for the eight novel complexes red-shift significantly from Ru3 to Ru12 as shown in Fig. 6. It is partly contributed from the narrower HOMO–LUMO gaps. The absorption band of Ru5 is 7 nm red-shifted comparing with that of Ru4 just because the two –CN groups are attached to different positions of the di-carboxyvinyl-bipyridine. The absorption intensity of Ru8 is obviously decreased comparing with those of Ru7 and Ru10 although they all contain four –CN groups. These two trends seem indicate that the higher density of the –CN

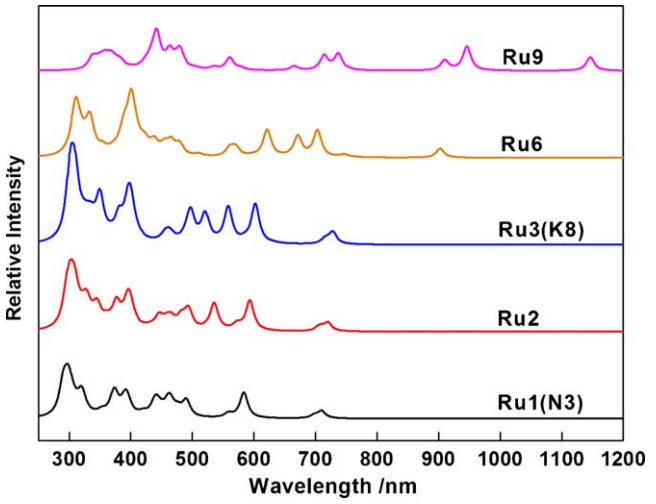

Fig. 5. Electronic absorption spectra of N3, K8 and three novel ruthenium sensitizers derived from N3.

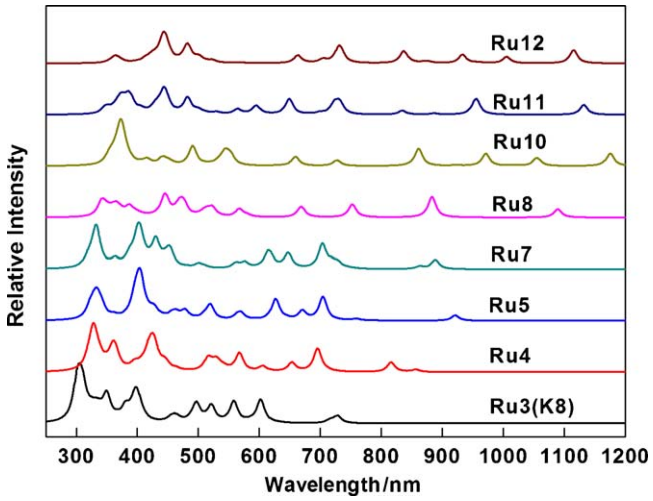

Fig. 6. Electronic absorption spectra of K8 and seven novel ruthenium sensitizers derived from K8.

groups is, the absorption intensities would be more decreased and the absorption positions more red-shifted. Ru3, Ru4, Ru10, Ru11 and Ru12 contain none, two, four, six, and eight –CN groups in their molecules, respectively, their absorption intensity decrease and absorption positions red-shift mostly along this order. The absorption range is found expanded while the absorption intensity decreased by increasing the numbers and density of –CN groups comparing the molecules above.

4. Conclusions

In summary, the novel ruthenium complexes except Ru2 have narrower HOMO–LUMO gap and their absorption positions are found red-shifted than those of N3 and K8, which indicates more light may be used in the photon-to-current conversion process. Their LUMO except that of Ru4 are much more moved to the acceptor moieties than those of N3 and K8, which indicates that more effective electron-separated states may be formed and more efficient electron injection may be obtained. The sensitizers Ru10 and Ru7 containing four –CN groups have wide absorption ranges and not weak absorption intensities, which are estimated to have the highest efficiencies in the current series of candidates. Increasing the numbers of the C=C double bonds between the carboxyl groups and the bipyridine ring seem to make the absorption intensity increase and the absorption positions red-shift. Increasing the numbers and densities of the –CN groups adjacent to the carboxyl groups seem to make the absorption positions red-shift while the absorption intensities decrease. If the sensitizer is designed to have an appropriate number of –CN groups and being attached to suitable positions using appropriate linker, higher conversion efficiency may be obtained. These results indicate that further developments in dye design will play an important role in the ongoing optimization of DSSC. Further experimental research on these novel ruthenium complex-sensitized solar cells is in progress in our group.

Acknowledgments

The authors thank the National Natural Science Foundation of China (Grant Nos. 20501011 and 20875042), National Basic Research Program of China (Grant Nos. 2011CB201600 and 2010CB234601), Tai-Shan Scholar Research Fund, and Key Lab of Novel Thin Film Solar Cells (KF200904), CAS, for financial support.

References

[1] M. Grätzel, Photoelectrochemical cells, Nature 414 (2001) 338–344.
[2] M. Grätzel, Dye-sensitized solar cells, J. Photochem. Photobiol. C 4 (2003) 145–153.
[3] M. Grätzel, Conversion of sunlight to electric power by nanocrystalline dye-sensitized solar cells, J. Photochem. Photobiol. A 164 (2004) 3–14.
[4] Md.K. Nazeeruddin, C. Klein, P. Liska, M. Grätzel, Synthesis of novel ruthenium sensitizers and their application in dye-sensitized solar cells, Coord. Chem. Rev. 249 (2005) 1460–1467.
[5] N. Robertson, Optimizing dyes for dye-sensitized solar cells, Angew. Chem. Int. Ed. 45 (2006) 2338–2345.
[6] F.T. Kong, S.Y. Dai, K.J. Wang, Review of recent progress in dye-sensitized solar cells, Adv. Optoelectr. (in press), doi:10.1155/2007/75384.
[7] H.J. Snaith, Estimating the maximum attainable efficiency in dye-sensitized solar cells, Adv. Funct. Mater. 20 (2010) 13–19.
[8] M.K. Nazeeruddin, A. Kay, I. Rodicio, R. Humphry-Baker, E. Müller, P. Liska, N. Vlachopoulos, M. Grätzel, Conversion of light to electricity by cis-X2bis(2,2′-bipyridyl-4,4′-dicarboxylate)ruthenium(II) charge-transfer sensitizers (X = Cl^-, Br^-, I^-, CN^-, and SCN^-) on nanocrystalline titanium dioxide electrodes, J. Am. Chem. Soc. 115 (1993) 6382–6390.
[9] A. Hagfeldt, M. Grätzel, Molecular photovoltaics, Acc. Chem. Res. 33 (2000) 269–277.
[10] M. Grätzel, Solar energy conversion by dye-sensitized photovoltaic cells, Inorg. Chem. 44 (2005) 6841–6851.
[11] Md.K. Nazeeruddin, S.M. Zakeeruddin, J.-J. Lagref, P. Liska, P. Comte, C. Barolo, G. Viscardi, K. Schenk, M. Grätzel, Stepwise assembly of amphiphilic ruthenium sensitizers and their applications in dye-sensitized solar cell, Coord. Chem. Rev. 248 (2004) 1317–1328.
[12] P. Wang, C. Klein, R. Humphry-Baker, S.M. Zakeeruddin, M. Grätzel, A high molar extinction coefficient sensitizer for stable dye-sensitized solar cells, J. Am. Chem. Soc. 127 (2005) 808–809.
[13] M.K. Nazeeruddin, T. Bessho, L. Ceveya, S. Itoa, C. Klein, F.D. Angelis, S. Fantacci, P. Comtea, P. Liska, H. Imai, M. Grätzel, A high molar extinction coefficient charge transfer sensitizer and its application in dye-sensitized solar cell, J. Photochem. Photobiol. A 185 (2007) 331–337.
[14] F. Gao, Y. Wang, D. Shi, J. Zhang, M. Wang, X. Jing, R. Humphry-Baker, P. Wang, S.M. Zakeeruddin, M. Grätzel, Enhance the optical absorptivity of nanocrystalline TiO_2 film with high molar extinction coefficient ruthenium sensitizers for high performance dye-sensitized solar cells, J. Am. Chem. Soc. 130 (2008) 10720–10728.
[15] F. Gao, Y. Wang, J. Zhang, D. Shi, M. Wang, R. Humphry-Baker, P. Wang, S.M. Zakeeruddin, M. Grätzel, A new heteroleptic ruthenium sensitizer enhances the absorptivity of mesoporous titania film for a high efficiency dye-sensitized solar cell, Chem. Commun. 23 (2008) 2635–2637.
[16] S. Wu, C. Chen, J. Chen, J. Li, Y. Tung, K. Ho, C. Wu, An efficient light-harvesting ruthenium dye for solar cell application, Dyes Pigments 84 (2009) 95–101.
[17] M.K. Nazeeruddin, P. Pechy, T. Renouard, S.M. Zakeeruddin, R. Humphry-Baker, P. Comte, P. Liska, L. Cevey, E. Costa, V. Shklover, L. Spiccia, G.B. Deacon, C.A. Bignozzi, M. Grätzel, Engineering of efficient panchromatic sensitizers for nanocrystalline TiO_2-based solar cells, J. Am. Chem. Soc. 123 (2001) 1613–1624.
[18] T. Renouard, R.A. Fallahpour, M.K. Nazeeruddin, R. Humphry-Baker, S.I. Gorelsky, A.B.P. Lever, M. Grätzel, Novel ruthenium sensitizers containing functionalized hybrid tetradentate ligands: synthesis, characterization, and INDO/S analysis, Inorg. Chem. 41 (2002) 367–378.
[19] C. Barolo, Md.K. Nazeeruddin, S. Fantacci, D. Di Censo, P. Comte, P. Liska, G. Viscardi, P. Quagliotto, F. De Angelis, S. Ito, M. Grätzel, Synthesis, characterization, and DFT–TDDFT computational study of a ruthenium complex containing a functionalized tetradentate ligand, Inorg. Chem. 45 (2006) 4642–4653.
[20] C.A. Mitsopoulou, I. Veroni, A.I. Philippopoulos, P. Falaras, Synthesis, characterization and sensitization properties of two novel mono and bis carboxyl-dipyrido-phenazine ruthenium(II) charge transfer complexes, J. Photochem. Photobiol. A. 191 (2007) 6–12.
[21] N. Onozawa-Komatsuzaki, M. Yanagida, T. Funaki, K. i Kasuga, K. Sayama, H. Sugihara, Near-IR sensitization of nanocrystalline TiO_2 with a new ruthenium complex having a 2,6-bis(4-carboxyquinolin-2-yl)pyridine ligand, Inorg. Chem. Commun. 12 (2009) 1212–1215.
[22] Md.K. Nazeeruddin, S.M. Zakeeruddin, R. Humphry-Baker, S.I. Gorelsky, A.B.P. Lever, M. Grätzel, Synthesis, spectroscopic and a ZINDO study of cis- and trans-(X_2)bis(4,4′-dicarboxylic acid-2,2′-bipyridine)ruthenium(II) complexes (X = Cl^-, H_2O, NCS^-), Coord. Chem. Rev. 208 (2000) 213–225.
[23] F. Aiga, T. Tada, Design of novel efficient sensitizing dye for nanocrystalline TiO_2 solar cell; tripyridine-thiolato (4,4′,4″-tricarboxyl-2,2′:6′,2″-terpyridine)ruthenium(II), Sol. Energy Mater. Sol. Cells 85 (2005) 437–446.
[24] T. Funaki, M. Yanagida, N. Onozawa-Komatsuzaki, K. Kasuga, Y. Kawanishi, H. Sugihara, A 2-quinolinecarboxylate-substituted ruthenium(II) complex as a new type of sensitizer for dye-sensitized solar cells, Inorg. Chim. Acta 362 (2009) 2519–2522.
[25] T. Bessho, E. Yoneda, J. Yum, M. Guglielmi, I. Tavernelli, H. Imai, U. Rothlisberger, Md.K. Nazeeruddin, M. Grätzel, New paradigm in molecular engineering of sensitizers for solar cell applications, J. Am. Chem. Soc. 131 (2009) 5930–5934.
[26] C. Klein, M.K. Nazeeruddin, P. Liska, D.D. Censo, N. Hirata, E. Palomares, J.R. Durrant, M. Grätzel, Engineering of a novel ruthenium sensitizer and its application in dye-sensitized solar cells for conversion of sunlight into electricity, Inorg. Chem. 44 (2005) 178–180.

[27] F.D. Angelis, S. Fantacci, A. Selloni, Time-dependent density functional theory study of the absorption spectrum of [Ru(4,4′-COOH-2,2′-bpy)$_2$(NCS)$_2$] in water solution: influence of the pH, Chem. Phys. Lett. 389 (2004) 204–208.
[28] F. De Angelis, S. Fantacci, A. Selloni, Md.K. Nazeeruddin, Time dependent density functional theory study of the absorption spectrum of the [Ru(4,4′-COO$^-$-2,2′-bpy)$_2$(X)$_2$]$^{4-}$ (X = NCS, Cl) dyes in water solution, Chem. Phys. Lett. 415 (2005) 115–120.
[29] M.K. Nazeeruddin, F.D. Angelis, S. Fantacci, A. Selloni, G. Viscardi, P. Liska, S. Ito, B. Takeru, M. Grätzel, Combined experimental and DFT–TDDFT computational study of photoelectrochemical cell ruthenium sensitizers, J. Am. Chem. Soc. 127 (2005) 16835–16847.
[30] Md.K. Nazeeruddin, Q. Wang, L. Cevey, V. Aranyos, P. Liska, E. Figgemeier, C. Klein, N. Hirata, S. Koops, S.A. Haque, J.R. Durrant, A. Hagfeldt, A.B.P. Lever, M. Grätzel, DFT-INDO/S modeling of new high molar extinction coefficient charge-transfer sensitizers for solar cell applications, Inorg. Chem. 45 (2006) 787–797.
[31] S. Ghosh, G.K. Chaitanya, K. Bhanuprakash, Md.K. Nazeeruddin, M. Grätzel, Electronic structures and absorption spectra of linkage isomers of trithiocyanato (4,4′,4″-tricarboxy-2,2′:6,2″-terpyridine) ruthenium(II) complexes: a DFT study, Inorg. Chem. 45 (2006) 7600–7611.
[32] R. Ma, P. Guo, H. Cui, X. Zhang, M.K. Nazeeruddin, M. Grätzel, Substituent effect on the meso-substituted porphyrins: theoretical screening of sensitizer candidates for dye-sensitized solar cells, J. Phys. Chem. A 113 (2009) 10119–10124.
[33] H. Cui, R. Ma, P. Guo, Q. Zeng, G. Liu, X. Zhang, Molecule design and screening of novel unsymmetrical zinc phthalocyanine sensitizers for dye-sensitized solar cells, J. Mol. Model. 16 (2010) 303–310.
[34] R. Ma, P. Guo, L. Yang, L. Guo, X. Zhang, Md.K. Nazeeruddin, M. Grtäzel, Theoretical screening of –NH$_2^-$, –OH$^-$, –CH$_3^-$, –F$^-$, and –SH$^-$ substituted porphyrins as sensitizer candidates for dye-sensitized solar cells, J. Phys. Chem. A 114 (2010) 1973–1979.
[35] R. Ma, P. Guo, L. Yang, L. Guo, Q. Zeng, G. Liu, X. Zhang, A theoretical interpretation and screening of porphyrin sensitizer candidates with anticipated good photo-to-electric conversion performances for dye-sensitized solar cells, J. Mol. Struct. THEOCHEM 942 (2010) 131–136.
[36] J.S. Binkley, J.A. Pople, W.J. Hehre, J. Am. Chem. Soc. 102 (1980) 939–947.
[37] P.J. Hay, W.R. Wadt, J. Chem. Phys. 82 (1985) 270–283.
[38] R. Ditchfield, W.J. Hehre, J.A. Pople, J. Chem. Phys. 54 (1971) 724–728.
[39] V. Shklover, Y.E. Ovchinnikov, L.S. Braginsky, S.M. Zakeeruddin, M. Grätzel, Chem. Mater. 10 (1998) 2533–2541.
[40] M. Cossi, G. Scalmani, N. Rega, V. Barone, New developments in the polarizable continuum model for quantum mechanical and classical calculations on molecules in solution, J. Chem. Phys. 117 (2002) 43–54.
[41] M.J. Frisch, G.W. Trucks, H.B. Schlegel, G.E. Scuseria, M.A. Robb, J.R. Cheeseman, J.A. Montgomery Jr., T. Vreven, K.N. Kudin, J.C. Burant, J.M. Millam, S.S. Iyengar, J. Tomasi, V. Barone, B. Mennucci, M. Cossi, G. Scalmani, N. Rega, G.A. Petersson, H. Nakatsuji, M. Hada, M. Ehara, K. Toyota, R. Fukuda, J. Hasegawa, M. Ishida, T. Nakajima, Y. Honda, O. Kitao, H. Nakai, M. Klene, X. Li, J.E. Knox, H.P. Hratchian, J.B. Cross, C. Adamo, J. Jaramillo, R. Gomperts, R.E. Stratmann, O. Yazyev, A.J. Austin, R. Cammi, C. Pomelli, J.W. Ochterski, P.Y. Ayala, K. Morokuma, G.A. Voth, P. Salvador, J.J. Dannenberg, V.G. Zakrzewski, S. Dapprich, A.D. Daniels, M.C. Strain, O. Farkas, D.K. Malick, A.D. Rabuck, K. Raghavachari, J.B. Foresman, J.V. Ortiz, Q. Cui, A.G. Baboul, S. Clifford, J. Cioslowski, B.B. Stefanov, G. Liu, A. Liashenko, P. Piskorz, I. Komaromi, R.L. Martin, D.J. Fox, T. Keith, M.A. Al-Laham, C.Y. Peng, A. Nanayakkara, M. Challacombe, P.M.W. Gill, B. Johnson, W. Chen, M.W. Wong, C. Gonzalez, J.A. Pople, Gaussian 03, Revision B.05, Gaussian, Inc., Pittsburgh, PA, 2003.
[42] H. Mizuseki, K. Niimura, C. Majumder, R.V. Belosludov, A.A. Farajian, Y. Kawazoe, C. Majumder, Theretical study of donor-spacer-acceptor structure molecule for stable molecular rectifier, Mol. Cryst. Liq. Cryst. 406 (2003), 11/[205]–17/[211].